ADVANCED MATERIALS

Nanoparticle-Induced Phase Transitions in Diblock-Copolymer Films**

By *Bumjoon J. Kim*, *Julia J. Chiu*, *Gi-Ra Yi*, *David J. Pine*, and *Edward J. Kramer**

Incorporation of nanoparticles into self-assembled block copolymers has been explored as an efficient way for improving the mechanical strength, electrical conductivity, and optical properties of materials at the nanometer scale. Recent computer simulations[1–3] predict that the cooperative self-organization of nanoparticles and block copolymers should yield a wide variety of structures with well-controlled particle arrangements. Such nanostructures may make it possible to fabricate novel functional materials, such as photonic bandgap materials, nanostructured solar cells, highly efficient catalysts, and high-density magnetic storage media. In particular, gold nanoparticles have attracted much interest for applications as catalysts[4,5] as well as building blocks for electronic devices that operate at the single-electron level.[6]

Over the years, several experimental methods have been developed for incorporating inorganic nanoparticles into polymeric nanostructures. These can be divided into two approaches. The first approach involves synthesizing nanoparticles in situ within preformed block-copolymer structures. Preformed micelles of block copolymers containing metal precursors are used as nanoreactors to synthesize nanoparticles selectively in block copolymers.[7–14] For example, Boontongkong et al.[7] produced micropatterned silver nanoparticles in a poly(styrene-*b*-acrylic acid) block-copolymer template using this approach. Such an approach is simple and can be easily extended to yield large-area samples. However, controlling the arrangement of the nanoparticles within the periodic structure of the block copolymer is difficult.

A second approach, recently proposed as a way to avoid some of the drawbacks of the method described above,[15–17] uses cooperative self-organization of nanoparticles and block copolymers. Based on theoretical predictions of the morphology of inorganic–organic hybrid materials by Balazs and co-workers,[3,18] Bockstaller et al.[15] demonstrated hierarchical pattern formation using block copolymers and binary mixtures of different sized hydrophobic nanoparticles. More recently, our previous work[19] showed how grafting different polymers to particle surfaces can be used to precisely control the placement of particles either at the center of one of the block-copolymer domains or at the interface dividing the two block-copolymer domains. This approach exploits enthalpic interactions between the block copolymer and functionalized nanoparticle surfaces to achieve precise particle placement.

Such precise control of nanoparticle position in block-copolymer thin films is important for developing highly organized hybrid materials. A particularly interesting example is the work of Russell and co-workers,[20] who showed that the orientation of block-copolymer domains in thin films could be controlled by introducing surface-active nanoparticles that preferentially segregated to the surface of high-surface-energy domains. However, the introduction of particles into block copolymers can also have profound effects on the overall morphology of nanocomposites, especially if the particle loading is high. Nevertheless, the effect of high particle loading on the overall composite morphology has not been explored in previous experimental studies.

In this communication, we report a nanoparticle-induced phase transition in a block-copolymer thin film as well as the formation of different structures of gold nanoparticles. When gold nanoparticles are coated with short polymer chains that are chemically identical to one of the copolymer blocks (in what follows we refer to such particles as simply Au particles, but it should be understood that in all cases they are coated with short polymer chains), the particles can self assemble near the center of that copolymer domain, as shown in Figure 1a. In this case, due to the coating of polystyrene (PS) chains on gold particles, the interaction between gold particles and one of the polymer blocks (PS) is neutral, but the interaction between the gold particles and the other block (P2 VP) is very unfavorable. In this report, we show that the lamellar morphology remains unchanged only if the gold nanoparticle volume fraction, c_{au}, is below some critical value, $c_{au,cr}$. For $c_{au} > c_{au,cr}$, the local concentration of gold nanoparticles varies along the thickness of the film, and different coexisting morphologies emerge as a function of sample depth.

For these experiments, symmetric block copolymers of polystyrene-*b*-poly(2-vinylpyridine) (PS-*b*-P2VP) with total molecular masses, M_n, of 59 kg mol^{-1} and 114 kg mol^{-1} were used. Gold nanoparticles with an average diameter of 2.5 nm were stabilized by short thiol end-functionalized PS chains (PS-SH; $M_n = 1.3$ kg mol^{-1}) that were grafted to the nanoparticle surfaces to make them compatible with the PS block and to prevent aggregation.

The transmission electron microscopy (TEM) image in Figure 1a shows the cross-sectional morphology of the film for $c_{au} = 0.14$ ($< c_{au,cr}$) cast from toluene. The lamellae lie parallel to the film surface, as expected. Since the P2VP was preferentially stained by iodine vapor, it appears darker than the PS in

[*] Prof. E. J. Kramer
Department of Materials, Department of Chemical Engineering
University of California
Santa Barbara, CA 93106 (USA)
E-mail: edkramer@mrl.ucsb.edu
B. J. Kim, Dr. J. J. Chiu, Dr. G.-R. Yi
Department of Chemical Engineering, University of California
Santa Barbara, CA 93106 (USA)
Prof. D. J. Pine
Department of Chemical Engineering, Department of Materials
University of California
Santa Barbara, CA 93106 (USA)

[**] This work was supported by the MRSEC Program of the National Science Foundation under award number DMR00-80034. We appreciate Dr. Huiman Kang and Dr. Kirill Katsov for valuable discussion.

  DOI: 10.1002/adma.200500502

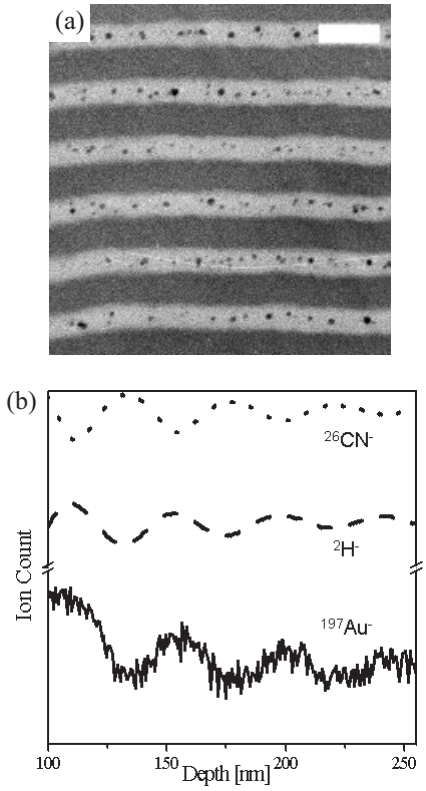

Figure 1. a) Cross-sectional TEM image of a film of gold particles/PS-*b*-P2VP ($M_n = 59$ kg mol^{-1}). The volume fraction of PS-coated gold particles is 0.14. Gold particles with 2.5 nm diameter are preferentially located near the center of the PS domains. Scale bar is 50 nm. b) A depth profile obtained from DSIMS. The solid, dashed, and dotted lines represent the signals of ions with masses 197, 2, and 26, respectively.

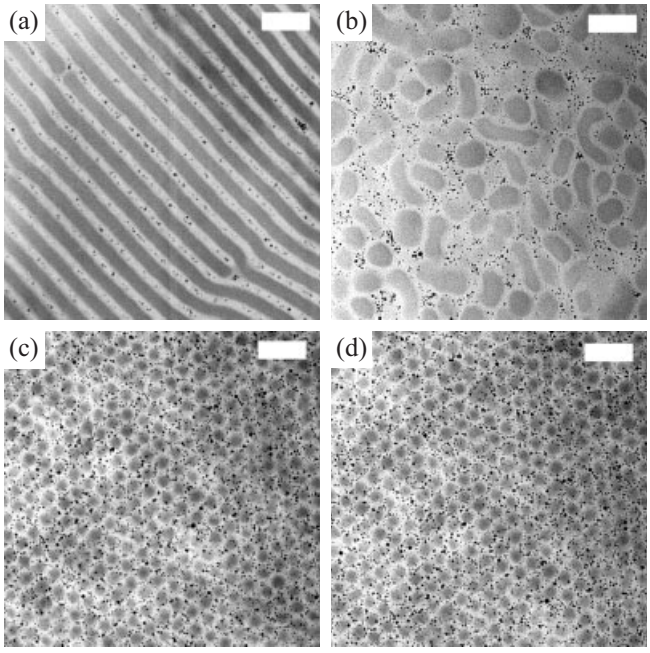

Figure 2. Cross-sectional TEM images of a film of gold particles/PS-*b*-P2VP ($M_n = 59$ kg mol^{-1}). The overall volume fraction of PS-coated gold particles is 0.5. The distance from the top of the film (L) is a) 27, b) 36, c) 52, and d) 95 μm. All scale bars are 100 nm.

bright-field TEM. The gold particles are aligned near the center of the PS domain, which has a domain size of 21 nm. The structure observed by TEM was confirmed by dynamic secondary ion mass spectrometry (DSIMS) experiments, a depth-profiling technique, in which the mass 2 signal ($^2H^-$), the mass 26 signal (CN^-), and the mass 197 signal (Au^-) were monitored as the film was sputtered away using a Cs^+ ion beam. The PS-*b*-P2VP used here has a deuterated PS block. The DSIMS peaks from the gold nanoparticles, which represent the PS block, in Figure 1b are coincident (i.e., in-phase) with those from deuterium, but are displaced (out-of-phase) from the P2VP peaks, indicating that the gold particles are located at the middle of the PS domain.

For $c_{au} > c_{au,cr}(\sim 0.25)$, we obtain dramatically different results. Instead of a single homogeneous lamellar phase, we observe layers with three distinct morphologies, as shown in Figure 2. Near the air–polymer interface, we observe a layer with lamellar morphology (Fig. 2a). Near the epoxy substrate, we observe a layer with spherical morphology, as shown in Figures 2c,d. Sandwiched between these two layers, we find a layer with disordered morphology (Fig. 2b). From the transmission electron micrographs in Figure 2, it is clear that most of the gold particles are located near the center of the PS domain, and that there is a greater concentration of particles in the spherical phase (Figs. 2c,d) than in the lamellar and disordered phases (Figs. 2a,b).

To study the relationship between the concentration of gold particles and the morphology of the film, we used the following procedure: TEM images at various depths of the film from the substrate (polymer/substrate interface) were taken from stained and unstained samples. Fractional gold core area coverage (dark spots) was determined for each TEM image using image analysis software. At each given depth of a film, the area fraction was obtained by averaging at least four TEM images. This area fraction of gold cores in the TEM images was converted into a local volume fraction of polymer-coated Au particles from our knowledge of the overall volume fraction of polymer-coated Au particles, which must equal the integral of the local volume fraction over the film thickness. The local volume fraction is plotted as a function of the distance from the bottom of the film in Figure 3a. Three main regions emerge from this analysis and can be identified in Figure 3a: 1) a low-particle-concentration region (~25 μm thick), with a nearly constant gold particle volume fraction of approximately 0.15; 2) a transitional region (~20 μm thick), with an increasing gold particle volume fraction between lamellar and hexagonal morphologies; and 3) a high-particle-concentration region (~60 μm thick), with a nearly constant gold particle volume fraction of approximately 0.65. The arrows pointing from labels (a–d) in Figure 3a identify the positions and concentrations corresponding to the TEM images shown in Figures 2a–d, respectively. TEM images at two different loca-

ADVANCED MATERIALS

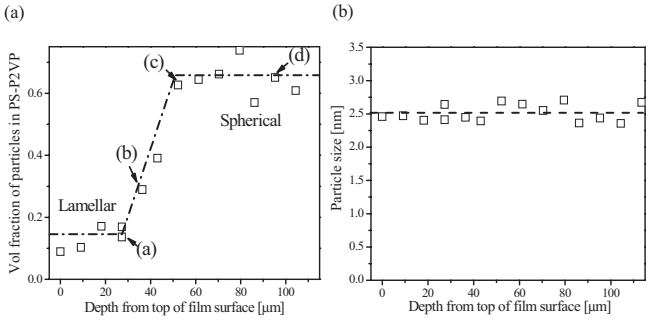

Figure 3. a) The volume fraction of polymer-coated gold particles, obtained from the TEM images in Figure 2 (labels (a)–(d) correspond to Figs. 2a–d, respectively), is shown as a function of the distance from the surface of the film, whose thickness is approximately 100 μm. The dashed line is a guide to the eye. b) The size of the gold core is shown at different film depths. It is constant approximately at 2.5 nm throughout the film.

tions, (c) and (d), within the high-particle-concentration regime show the same spherical morphology and have approximately the same concentration of gold particles, as do all cuts within this region. Similarly, the concentration of gold particles is approximately constant for all cuts within the region with lamellar morphology. Thus, we observe a two-phase macrostructure having a layer of low particle volume fraction with a lamellar morphology near the air/film interface and a layer of high particle volume fraction with a spherical morphology near the substrate. We also find that the mean gold-particle size has a constant value of approximately 2.5 nm along the thickness of the film as indicated by a flat profile in Figure 3b.

To investigate the mechanisms that drive the morphological changes of block copolymer in the composite film, two different control experiments were performed. First, a PS-*b*-P2VP film was prepared exactly as before but without gold particles. As expected, only the lamellar morphology was observed from the top to the bottom of the film. Second, a PS-*b*-P2VP film was prepared as before but with PS-SH polymers replacing the gold nanoparticles. The amount of PS-SH was chosen to correspond to the same volume fractions that were used in the PS-coated Au/PS-*b*-P2VP composites. The PS-SH was observed to swell the PS domains selectively in the PS-*b*-P2VP films and caused the block copolymers to adopt spherical micellar morphology instead of the lamellar morphology observed without the PS-SH. However, in this case the spherical morphology was observed homogeneously throughout the film; no spatially varying morphologies were observed for control samples prepared without PS-coated gold nanoparticles. Therefore, we conclude that PS-functionalized gold particles behave like PS homopolymers and that the observed morphological changes for the concentrations examined arise from the spatially varying concentration of nanoparticles.

To further examine these phenomena, experiments were performed with longer symmetric block copolymers of PS-*b*-P2VP (M_n = 114 kg mol^{-1}) using THF as a solvent. For a somewhat lower overall volume fraction of gold particles (0.30), we observed a similar two-phase macrostructure: near the surface, the film was lamellar with low particle concentration; near the substrate, the film was hexagonal with high particle concentration (Fig. 4). As before, particles and diblock copolymers form layered structures with three distinctive concentration regions and three different morphologies as a function of the depth of film. Based on these experimental observations, we present a simplified schematic of the two-phase macrostructure of polymer/gold particles in Figure 4d.

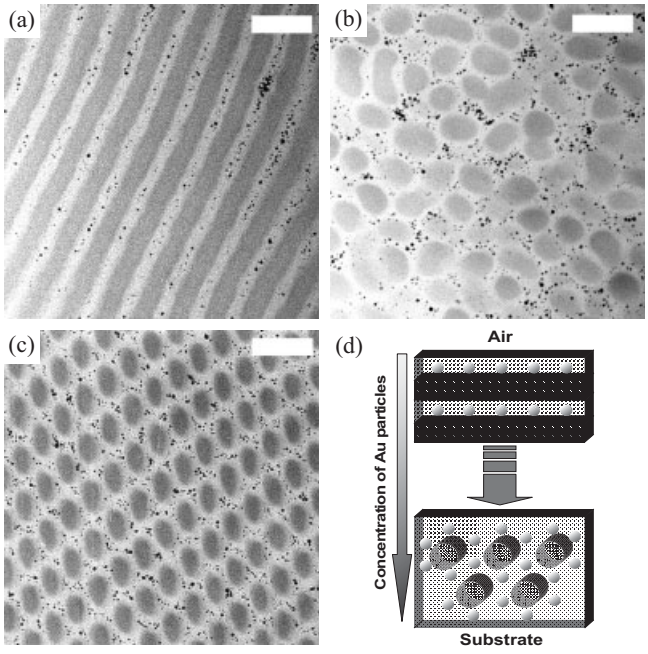

Figure 4. Cross-sectional TEM image of a film of gold particles/PS-*b*-P2VP (M_n = 114 kg mol^{-1}) with an overall volume fraction of polymer-coated Au particles of 0.3. Distance from the top of film (*L*) is a) 27, b) 46, c) 64 μm. All scale bars are 100 nm. d) A schematic of the film structure based on the TEM images (a)–(c). A two-phase macrostructure is observed, with the surface layers of the film being lamellar with low particle concentration and the substrate layers being hexagonal with high particle concentration.

To our knowledge, the observed gradient in the concentration of gold particles in a polymer composite film has not been reported previously, nor have there been any mechanisms proposed to explain such phenomena. Here we offer some insights that may help explain our observations. First, we can rule out gravitational settling of the gold particles. Even though the density of gold (= 19.3 g cm^{-3}) is much greater than the densities of PS and P2VP (= 1.0 g cm^{-3}), the small size of the gold particles assures that the gravitational energy, given by Δmgh (where Δm is the mass of a gold nanoparticle less the mass of the fluid it displaces, g is acceleration due to gravity, and h is the height of the film) is much less than the thermal energy, k_BT (where k_B is the Boltzmann constant and T is temperature). In fact, the gravitational height obtained by

setting $\Delta mgh = k_B T$ is approximately 2.8 m for 2.5 nm gold nanoparticles in PS-*b*-P2VP, which means that gravity is irrelevant over the micrometer length scales corresponding to the thicknesses of the films considered here. Furthermore, TEM analysis reveals that gold nanoparticle size does not vary with film depth.

The fact that the variation in morphology and concentration of gold particles has been observed only in solvent-cast samples may provide a clue to the mechanisms that produce the unique phase coexistence we observe. Therefore, we consider the interactions between gold particles and polymers during solvent evaporation. When the sample is cast, there is an ample amount of solvent present. As the sample anneals, however, solvent evaporates from the top of film. Because of the lower concentration of solvent, we believe that a condensed polymer structure nucleates at the air/film interface. Moreover, as the concentration of solvent decreases, the sample near the air/film interface passes through its glass-transition temperature (T_g), since T_g for the pure polymer is well above the sample processing temperature. This surface-drying picture is supported by previous reports that show the concentration of solvent at the top surface of the film is lower than that near the bottom of the film.[21,22] Because the surface energy of PS at the air/sample interface is lower than that of P2VP,[23,24] the lamellar morphology is formed with the PS block at the air/polymer interface. Once the lamellar structure is formed from the surface, it propagates into the film forming alternating layers of PS and PVP, pushing the majority of gold particles towards the substrate. Several processes can possibly contribute to the transport of gold towards the substrate: 1) the diffusion of gold particles towards the substrate is faster than the diffusion away from the substrate because there is more solvent near the substrate; 2) the interaction between PS-coated particles and solvent (toluene or tetrahydrofuran (THF)) is more favorable than that between solvent and PS-*b*-P2 VP; and 3) the lamellar layers formed near the sample/air interface cannot accommodate a large volume fraction of PS-coated gold particles and maintain the lamellar morphology. As particles concentrate toward the bottom of the film, the morphology changes from lamellar to morphologies that can better accommodate having PS as the major component. This occurs when the concentration of gold particles exceeds a critical value, since, as discussed previously, PS-coated gold particles behave as homopolymers that swell the PS domains of the PS-*b*-P2VP block copolymer. At some point during the evaporation process, the sample becomes kinetically frozen so that the particles can no longer redistribute themselves due to the very low mobility of gold particles in the solvent-poor environment. Thus, a spatially varying morphology in a single film can result from a non-equilibrium process caused by slow solvent evaporation and by favorable interaction between solvent and gold particles.

The choice of solvent and film thickness can also be critical factors for producing a particle-concentration gradient. When a volatile, non-selective solvent for PS and P2VP, such as dichloromethane, was used for sample preparation, the spatially varying morphology was not observed. Thus, selectivity and/or volatility of the solvent may be important in forming a particle-concentration gradient. Even using toluene, no spatial variation of morphology was observed for films less than 20 μm thick, which is the length scale of the transition regime between lamellar and hexagonal phases. Even though these phenomena occur out of equilibrium, they may be useful for applications, as various morphologies with different length scales can be obtained in a single film simply by controlling the solvent and annealing conditions. Further experiments investigating the cause of gold-nanoparticle-concentration gradients and the roles of solvent and molecular mass of PS-*b*-P2VP and PS-SH for the inorganic–organic nanocomposite materials are underway.

In summary, we have observed morphological changes and a layered order–order transition in block copolymer films that are caused by introducing high concentrations of surface-modified gold nanoparticles into one of the diblock domains. The versatility of the method opens up possibilities for building a variety of self-assembled structures of inorganic nanoparticles in a single step at low cost.

Experimental

Synthesis of Gold Particles Stabilized by Thiol-Terminated PS: Thiol-terminated PS (PS-SH) was synthesized by living anionic polymerization using benzene as solvent at 30 °C [25]. First, polymerization of styrene was initiated by *sec*-butyl lithium and was polymerized for 3 h under nitrogen. Polystyryl anions were titrated by propylene sulfide, and polymers were protonated by acidic methanol. The molecular mass, M_n, and polydispersity index of PS-SH were 1.3 kg mol^{-1} and 1.10, respectively. Gold nanoparticles with diameter $d = 2.5$ nm and stabilized by the thiol-terminated PS were synthesized using a procedure as described by Brust et al. [26]. Gold nanoparticles were washed in a mixture of ethanol and toluene.

Preparation of Hybrid Gold Particles/PS-b-P2VP Samples: Two kinds of PS-*b*-P2VP with different M_n were used for this study. The total M_n and polydispersity of the first PS-*b*-P2VP was 59 kg mol^{-1} and 1.05, respectively, which was made by living anionic polymerization at University of California Santa Barbara (UCSB). The weight fraction of PS block was 0.51. Another PS-*b*-P2VP with a PS-block weight fraction of 0.50, a polydispersity of 1.08, and a higher M_n (114 kg mol^{-1}) was purchased from Polymer Source Inc. Typically, a 5 wt.-% polymer solution in toluene or THF admixed with PS-coated gold particles was prepared. Particle/polymer composite material was prepared by solvent casting onto an epoxy substrate. The mixture of nanoparticles and polymer was annealed in a saturated solvent atmosphere at 55 °C. The solvent annealing time was usually three days, followed by one day of slow drying in air, and further removal of solvent under vacuum for an additional minimum of 8 h.

Preparation of Samples for Cross-Sectional TEM: The sample was embedded into an epoxy mold and microtomed at room temperature into 30 nm thick films using a diamond knife with a Leica Ultracut microtome. To investigate the cross-sectional morphology of the films, the microtomed samples were stained with iodine vapor for 7–10 h. The morphology was investigated using FEI T20 TEM at an accelerating voltage of 200 keV.

Received: March 10, 2005
Final version: June 13, 2005
Published online: September 15, 2005

ADVANCED MATERIALS

[1] J. Y. Lee, R. B. Thompson, D. Jasnow, A. C. Balazs, *Faraday Discuss.* **2003**, *123*, 121.
[2] J. Y. Lee, R. B. Thompson, D. Jasnow, A. C. Balazs, *Macromolecules* **2002**, *35*, 4855.
[3] R. B. Thompson, V. V. Ginzburg, M. W. Matsen, A. C. Balazs, *Science* **2001**, *292*, 2469.
[4] M. Haruta, *Catal. Today* **1997**, *36*, 153.
[5] T. F. Jaramillo, S. H. Baeck, B. R. Cuenya, E. W. McFarland, *J. Am. Chem. Soc.* **2003**, *125*, 7148.
[6] D. L. Feldheim, K. C. Grabar, M. J. Natan, T. E. Mallouk, *J. Am. Chem. Soc.* **1996**, *118*, 7640.
[7] Y. Boontongkong, R. E. Cohen, *Macromolecules* **2002**, *35*, 3647.
[8] L. H. Bronstein, S. N. Sidorov, P. M. Valetsky, J. Hartmann, H. Colfen, M. Antonietti, *Langmuir* **1999**, *15*, 6256.
[9] R. S. Kane, R. E. Cohen, R. Silbey, *Chem. Mater.* **1999**, *11*, 90.
[10] V. Sankaran, J. Yue, R. E. Cohen, R. R. Schrock, R. J. Silbey, *Chem. Mater.* **1993**, *5*, 1133.
[11] B. H. Sohn, J. M. Choi, S. I. Yoo, S. H. Yun, W. C. Zin, J. C. Jung, M. Kanehara, T. Hirata, T. Teranishi, *J. Am. Chem. Soc.* **2003**, *125*, 6368.
[12] B. H. Sohn, B. H. Seo, *Chem. Mater.* **2001**, *13*, 1752.
[13] J. Spatz, S. Mossmer, M. Möller, M. Kocher, D. Neher, G. Wegner, *Adv. Mater.* **1998**, *10*, 473.
[14] E. H. Tadd, J. Bradley, R. Tannenbaum, *Langmuir* **2002**, *18*, 2378.
[15] M. R. Bockstaller, Y. Lapetnikov, S. Margel, E. L. Thomas, *J. Am. Chem. Soc.* **2003**, *125*, 5276.
[16] K. Tsutsumi, Y. Funaki, Y. Hirokawa, T. Hashimoto, *Langmuir* **1999**, *15*, 5200.
[17] C. C. Weng, K. H. Wei, *Chem. Mater.* **2003**, *15*, 2936.
[18] R. B. Thompson, V. V. Ginzburg, M. W. Matsen, A. C. Balazs, *Macromolecules* **2002**, *35*, 1060.
[19] J. J. Chiu, B. J. Kim, E. J. Kramer, D. J. Pine, *J. Am. Chem. Soc.* **2005**, *127*, 5036.
[20] Y. Lin, A. Böker, J. He, K. Sill, H. Xiang, C. Abetz, X. Li, J. Wang, T. Emrick, S. Lung, Q. Wang, A. Balazs, T. P. Russell, *Nature* **2005**, *434*, 55.
[21] G. Kim, M. Libera, *Macromolecules* **1998**, *31*, 2569.
[22] S. H. Kim, M. J. Misner, T. Xu, M. Kimura, T. P. Russell, *Adv. Mater.* **2004**, *16*, 226.
[23] G. Coulon, T. P. Russell, V. R. Deline, P. F. Green, *Macromolecules* **1989**, *22*, 2581.
[24] H. Yokoyama, E. J. Kramer, M. H. Rafailovich, J. Sokolov, S. A. Schwarz, *Macromolecules* **1998**, *31*, 8826.
[25] J. M. Stouffer, T. J. McCarthy, *Macromolecules* **1988**, *21*, 1204.
[26] M. Brust, M. Walker, D. Bethell, D. J. Schiffrin, R. Whyman, *J. Chem. Soc. Chem. Commun.* **1994**, 801.

Nanoporous, Ultralow-Dielectric-Constant Fluoropolymer Films from Agglomerated and Crosslinked Hollow Nanospheres of Poly(pentafluorostyrene)-*block*-Poly(divinylbenzene)

By *Guo-Dong Fu*, *Zhenhua Shang*, *Liang Hong*, *En-Tang Kang*,* and *Koon-Gee Neoh*

Ultralow dielectric constant (κ) interlayers with $\kappa < 2.0$ are required to reduce the resistance–capacitance (RC) time delay, cross talk, and power dissipation in the new generation of submicrometer- and nanometer-sized electronics.[1–6] Inclusion of air ($\kappa \sim 1.0$) in interconnect structures[7,8] and incorporation of nanopores into polymers[9–11] are attractive approaches to reducing the dielectric constants of materials. The preparation of nanoporous low-κ poly(silsesquioxane)s[12–15] and polyimides[16–20] from their copolymers with thermally labile block or graft chains has been reported. Fluoropolymers are potential candidates for interlayer dielectric applications because they have good chemical and thermal stability and the lowest dielectric constants among the bulk polymers.[5,21] It is possible to obtain ultralow-κ materials with κ-values less than 2.0 by introducing nanopores into fluoropolymer films.[22–24]

In the present work, we report on an alternative approach to fabricating crosslinked nanoporous fluoropolymer films with $\kappa \sim 1.7$. The synthesis strategy is shown schematically in Figure 1. First, the initiator for atom-transfer radical polymerization (ATRP), trichloro(4-chloromethyl-phenyl)silane, is immobilized on the surface of SiO_2 nanoparticles of about 25 nm in diameter. Consecutive surface-initiated ATRP reactions of pentafluorostyrene (PFS) and divinylbenzene (DVB) give rise to SiO_2 nanoparticles with surface-grafted poly(pentafluorostyrene)-*block*-poly(divinylbenzene) (SiO_2-*g*-PFS-*b*-PDVB). SiO_2-*g*-PFS-*b*-PDVB nanospheres of about 80–150 nm in diameter are allowed to agglomerate on a silicon substrate to form a film of about 2–4 μm in thickness. Under UV irradiation, the PDVB outer layer with residual double bonds on the core–shell nanospheres undergoes inter- and intrasphere crosslinking to strengthen the film. Removal of the silica cores of the crosslinked nanospheres by HF etching gives rise to the nanoporous fluoropolymer film. The high porosity is due to both the interstitial spaces between the nanospheres and the hollow cores of the nanospheres, and leads to a dielectric constant as low as 1.7 for the resulting film.

[*] Prof. E.-T. Kang, G.-D. Fu, Z. Shang, Prof. L. Hong
Prof. K.-G. Neoh
Department of Chemical and Biomolecular Engineering
National University of Singapore
Kent Ridge, Singapore 119260 (Singapore)
E-mail: cheket@nus.edu.sg

  DOI: 10.1002/adma.200500762